

EVALUATION OF CRACKING AND DEFORMATION BEHAVIOR OF RC BEAMS REINFORCED WITH HIGH STRENGTH REBAR

Usman Farooq^{*1}, Hikaru Nakamura^{*2}, Yamamoto Yoshihito^{*3}, Taito Miura^{*4}

ABSTRACT

This paper evaluated the effect of high strength rebar of SD685 on the cracking and deformation behavior. Four specimens with alternative combination of either SD345 or SD685 rebar along with either 30MPa or 70MPa concrete strength were experimentally tested and result were compared with the equations in JSCE design standards about crack width, crack space and deformation behavior. To build comparative analytical study, 3D Rigid Body Spring Model (RBSM) was used and experimental results were validated. Extensive parametric study considering various reinforcement ratios and concrete covers was also conducted analytically by using RBSM and the applicability of JSCE equations was confirmed.

Keywords: high strength rebar, crack width, crack space, curvature, RBSM

1. INTRODUCTION

In order to design reasonable RC member sizes for the required loading capacity with normal strength rebar, the heavy congestion of tensile reinforcement may occur, that often results into lower workability and poor quality control. Furthermore, the strength of the members is not significantly higher. In this scenario, utilization of high strength rebar can mitigate all these problems related to designing and intensive labor work as it provides many merits such as smaller cross-sections, avoidance of heavy reinforcing bar congestion and improvement of member strength and so on. Considering these advantages, the utilization of high strength rebar has significantly increased in recent years.

In order to utilize the merits, many researches have been conducted to investigate flexural strength and ductility achieved due to high strength rebar in RC members. These studies contribute to avoid congestion of rebar, achieve higher ductility and design high rise pier and buildings [1, 2]. However, the knowledge about crack width and deformation is still limited [3], that are important design parameters in serviceability conditions [4, 5]. Moreover, the usage of high strength rebar also requires to modify the limitation of design guidelines regarding serviceability condition because the limitation of rebar strength in JSCE design standards is SD490 [3].

This study investigated cracking and deformation behavior for RC beams designed in flexure with high strength rebar SD685 experimentally and analytically. In the experimental study, four beams were tested by considering strength combination of rebar and concrete. In the numerical study, RBSM was used to simulate tested specimen and the effect of longitudinal reinforcement ratio and concrete cover on cracking

width and deformation behavior was investigated under parametric study. Moreover, the applicability of design equation for crack width and deformation given by JSCE standards was verified.

2. BENDING TEST OF RC BEAMS WITH HIGH STRENGTH REBAR

2.1 Outline of test specimen

For the sake of comparative studies to consider the influence of high strength rebar on cracking and deformation behavior, four beams were constructed by using either SD345 or SD685 rebar. Concrete compressive strength was also changed, which were 33.70 and 76.45 MPa. Because when high strength rebar is used, high strength concrete is often combined to consider advantage of high strength material. Properties of materials are provided in Table 1. CN and CH are designations for normal and high strength concrete, while SN and SH are designations for normal and high strength rebar.

Table 1 Properties of materials

Beam	Concrete		Rebar	
	f_c' (MPa)	E_c (GPa)	f_y (MPa)	E_s (GPa)
CN-SN	33.70	26.10	365.00	197.20
CN-SH			721.00	193.20
CH-SN	76.45	34.50	365.00	197.20
CH-SH			721.00	193.20

Fig. 1 shows the outline of specimen. The cross-sectional dimensions of all specimen are 200mm width and 300mm height along with 40mm concrete cover. As

*1 Dept. of Civil Engineering, Nagoya University, JCI Student Member

*2 Prof., Dept. of Civil Engineering, Nagoya University, Dr.E., JCI Member

*3 Associate Prof., Dept. of Civil Engineering, Nagoya University, Dr.E., JCI Member

*4 Assistant Prof., Dept. of Civil Engineering, Nagoya University, Dr. Ph., JCI Member

tensile reinforcement, two D16 rebars are provided and reinforcement ratio is kept 0.77%. In all specimen, 2 two D10-SD345 rebars are arranged as compressive reinforcement. While to achieve flexural failure, shear reinforcement was also provided with varying spacing as per flexural failure load requirement.

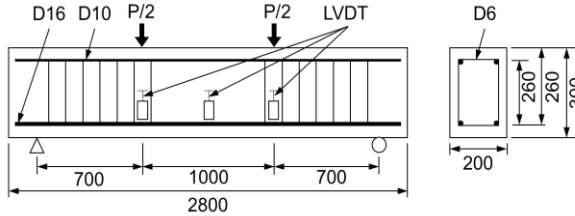


Fig. 1 Outline of test specimen

To understand the flexural behavior in a better way, four point bending test was performed and a constant moment span of 1m was provided along with two points loading at the mid span. In order to evaluate cracking behavior, beams were loaded until the initiation of cracks and then unloaded. After unloading, Pi-shape gauges were installed across cracks to measure crack width at several progressive loading stages and cracking pattern was also marked. While to obtain displacement, three displacement transducers were used at center point and loading points of specimen. The data obtained from these transducers was used to calculate moment-curvature.

2.1 Test results

2.1.1 Load-Displacement relationship

Fig. 2 shows load-displacement relationship for all four beams. In the figures, the black, green, blue and red solid and dashed lines show experimental and analytical results, respectively. The analytical results will be discussed in chapter 3.

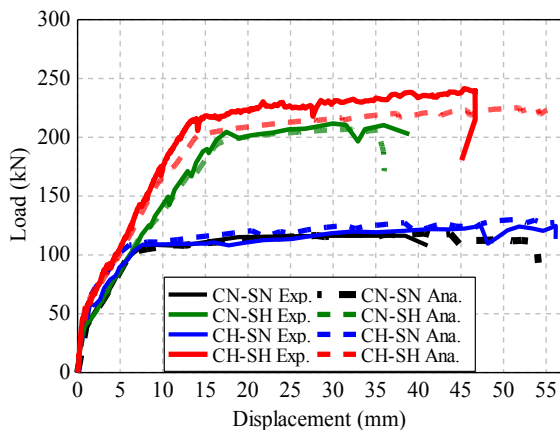


Fig. 2 Load-Displacement Relationship

For the beams with SD685, observed yield load and yield displacement are two times of beams with SD345. The curves of beam with SD345 show almost same yielding points. While for the beams with SD685 different stiffness and yielding points are observed depending upon the combination of concrete compressive strength. Specimen with combination high

strength concrete and high strength rebar sustained slightly larger load.

2.2.2 Cracking Pattern

In Figs. 3~6, at the left hand side experimentally observed cracking pattern for beams CN-SN, CN-SH, CH-SN and CH-SH at several loading stages within constant moment span is shown respectively. In case of experiments, different colors of crack represent the initiation of cracks at progressive loading stages. Maximum allowed crack space calculated at yielding load by Eq. (1), which is part of JSCE equation for maximum crack width [3], is also shown in Table 2. In all the figures, location of maximum crack space is indicated by the arrows between the corresponding cracks.

$$L_{max} = 1.1 k_1 k_2 k_3 (4c + 0.7(c_s - \Phi)) \quad (1)$$

where, k_1 , k_2 and k_3 represent surface geometry of rebar, quality of concrete and No. of layer of tensile reinforcement respectively. While c , c_s and Φ represent concrete cover, center to center distance and diameter of tensile reinforcement respectively.

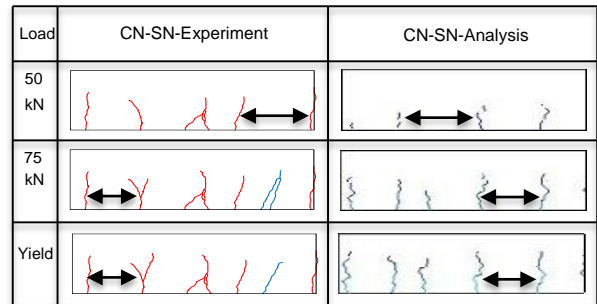


Fig 3. Crack pattern for beam CN-SN in case of experiment and analysis

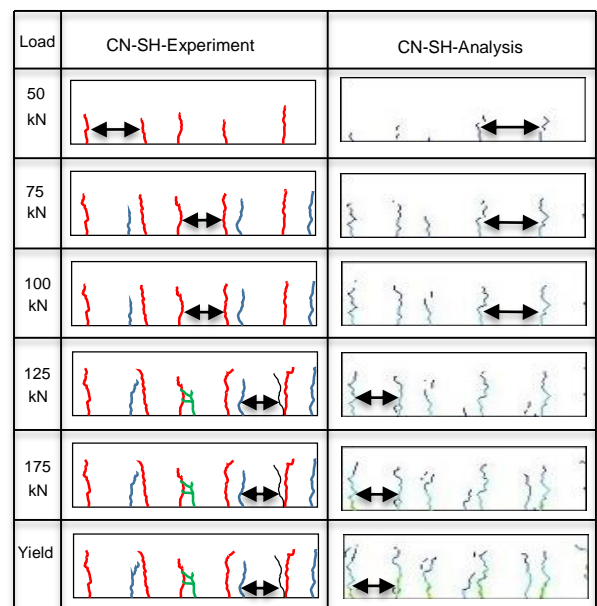


Fig 4. Crack pattern for beam CN-SH in case of experiment and analysis

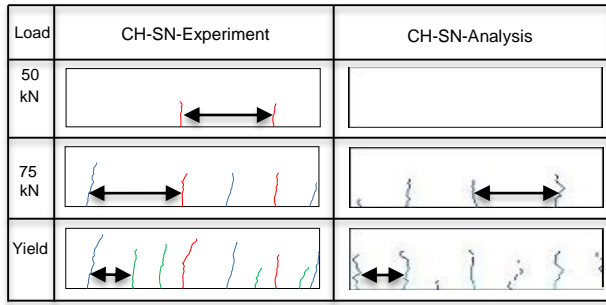


Fig 5. Crack pattern for beam CH-SN in case of experiment and analysis

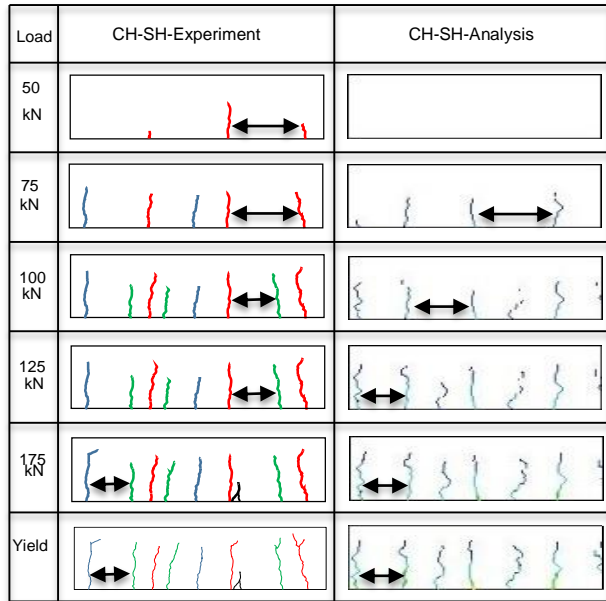


Fig 6. Crack pattern for beam CH-SH in case of experiment and analysis

Table 2 Maximum crack space in case of experiments, analysis and JSCE equation

Case	Max. crack space (mm)		
	Experiments	Analysis	JSCE eq. (L_{max})
CN-SN	240	235	239
CN-SH	180	170	239
CH-SN	185	180	208
CH-SH	185	178	208

Maximum crack space of beam CN-SN is similar with the JSCE equation. Beam CH-SN shows smaller maximum crack space due to the effect of concrete strength. For the beams with SD685, few new cracks initiated at loading stages higher than yielding load of the beams with SD345. Therefore the crack space for beams with SD685 became smaller at progressive loading stages. We observed that the usage of high strength rebar with normal and high strength concrete causes smaller values of maximum crack space, but the influence of concrete strength is not significant.

2.2.3 Change in maximum crack width

Figs. 7 and 8 show the change of maximum crack width in case of beams with normal and high strength concrete respectively. JSCE design standard provides design equation for maximum crack width as show in Eq. (2) [3]. Design values of maximum crack width are obtained from Eq. (2), in which the time-dependent effect of ϵ'_{csd} is neglected, because the tests were conducted in a short time just after curing.

$$w = 1.1 k_1 k_2 k_3 (4c + 0.7(c_s - \Phi)) \left(\frac{\sigma_{se}}{E_s} + \epsilon'_{csd} \right) \quad (2)$$

where, σ_{se} represents stress level of rebar at any loading stage, E_s is modulus of elasticity of steel and ϵ'_{csd} represents creep and shrinkage effect.

Design values are shown by orange colored dashed and solid lines for normal and high strength concrete, respectively. Although concrete strength influences the crack width, the effect of high strength concrete for the beams with SD345 and SD685 is quite similar. The changes of crack width for the beams with SD685 show almost linear increase until yielding load. This means that larger strain and stress levels of SD685 do not affect the crack width significantly. Moreover, maximum crack width obtained from design equation ensured the safety side value of maximum crack width until near the yield load for all the combinations.

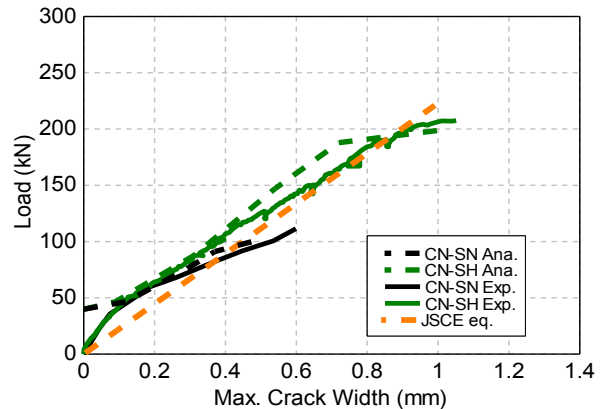


Fig. 7 Change in maximum crack width in case of normal strength concrete

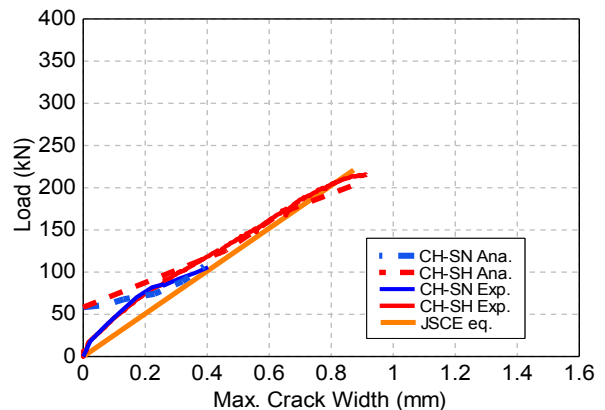


Fig. 8 Change in maximum crack width in case of high strength concrete

2.2.4 Deformation behavior

Figs. 9 and 10 show the moment and average curvature relationship within constant moment span for beams with normal and high strength concrete, respectively. Only one LVDT at center was used in case of beam CN-SN, so representative moment-curvature curve could not be obtained. Design values obtained from Eq. (3) [3] are also shown by orange colored dashed and solid lines for normal and high strength concrete, respectively.

$$I_e = \left(\frac{M_{cr}}{M_d}\right)^3 (I_g) + \left(1 - \left(\frac{M_{cr}}{M_d}\right)^3\right) I_{cr} \quad (3)$$

where, I_{cr} and M_{cr} are moment of inertia and moment at cracking loading, I_e and M_d represents moment of inertia and moment at loading stages higher than the cracking load and I_g is gross moment of inertia of cross-section.

Trend of moment curvature graphs for beams with SD685 shows linear behavior until yield load after cracking, which shows that higher stress and strain levels do not affect curvature. The curves are identical with design values for both high and normal strength concrete. However, the moment-curvature graph of specimen CH-SN shows slightly lower stiffness after cracking as compared to design values.

3. EVALUATION OF CRACKING AND DEFROMATION BEHAVIOR WITH RBSM

3.1 Outline of analysis

In order to simulate beam behavior, 3-D RBSM was applied. RBSM is a powerful tool to simulate not only macro behavior such as load-displacement relationship but also local behavior such as crack width, because it is based on discrete element method [6]. In RBSM, concrete is modeled as an assemblage of rigid particle interconnected by spring at their boundary surfaces as shown in Fig. 11. Since crack propagation is affected by mesh design, a random geometry is generated by Voronoi tessellation to reduce mesh bias on the development of potential crack. Moreover, beam elements are attached to concrete by zero-size link element, which provides a load-transfer mechanism between concrete particles and beam element [7]. The parameters and constitutive models applied in RBSM can be referred in the research by Yamamoto et al. [6, 8]. In these research papers, parameters in RBSM were calibrated based on many experimental results. The bond stress slip relationship is based on Eq. (4) derived from Suga et al. model [9], in which effect of concrete strength is considered.

$$\tau = 0.4 \times 0.90 (f_c')^{\frac{2}{3}} \left(1 - \exp\left(40\left(-40\left(\frac{s}{D}\right)^{0.5}\right)\right)\right) \quad (4)$$

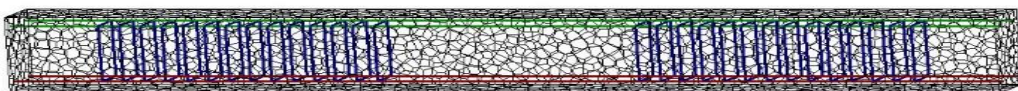


Fig. 12 Numerical model for test beam CN-SN

where, D is the diameter and s is slippage of reinforcement.

The analytical model of the test specimen CN-SN can be seen in Fig. 12. The same material properties of concrete and reinforcing bars are utilized as shown in Table 1. While average mesh size is about 30mm.

3.2 Comparison of analytical results with test results

Fig. 2 also shows load-displacement relationship in case of analysis as compared to experiments. In case of analysis, the black, green, blue and red dashed lines show results for analytical specimen. The load-displacement relationship is similar with test results. Overall flexural failure is observed for all beams in case of analysis as compared to experiments.

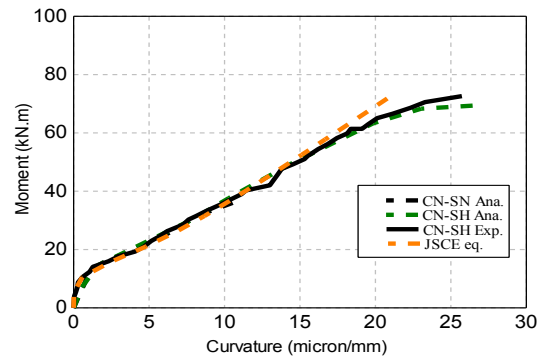


Fig. 9 Moment-Curvature relationship in case of normal strength concrete

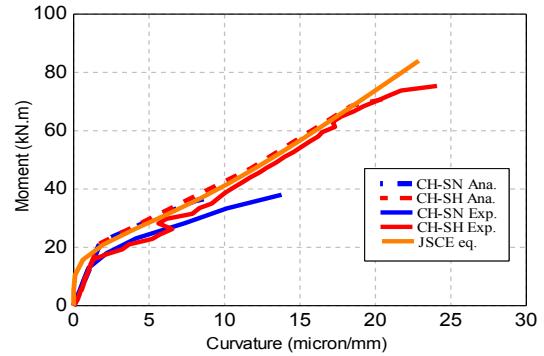


Fig. 10 Moment-Curvature relationship in case of high strength concrete

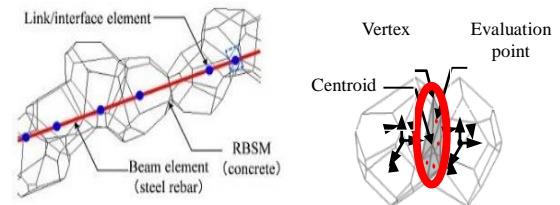


Fig. 11 RBSM

Fig. 3~6 show analytically observed cracking pattern for beams CN-SN, CN-SH, CH-SN and CH-SH respectively. In case of all the beams, during subsequent loading stages, almost similar cracking space has been observed in comparison of analysis to experiments.

In case of analysis, change in maximum crack width is shown in Figs. 7 and 8 along with experimental results. As looked at these figures, it can be said that this analysis can reconstruct the change in maximum crack width even though concrete or rebar strength are different.

Considering deformation behavior, Figs. 9 and 10 provides results for analysis as compared to experiments. In all the cases, analytically observed moment-curvature is in very good agreement with experimental results.

3.3 Evaluation of several design parameters

JSCE's eq. (2) for maximum crack width comprises of several design factors including reinforcement ratio (ρ_t), concrete cover (c), and so on. In order to extensively evaluate the effect of high strength rebar (SD685) on change in maximum crack width and deformation, several cases of reinforcement ratio and concrete cover are discussed in parametric study and results are obtained analytically by using RBSM. $\rho_t=0.51\%$ (D10), $\rho_t=0.77\%$ (D16), $\rho_t=1.33\%$ (D21) and $\rho_t=1.89\%$ (D25) cases are discussed to evaluate the effect of reinforcement ratio, in all cases 2 rebar are provided as tensile reinforcement.

Cases of $c=20\text{mm}$, $c=40\text{mm}$ and $c=60\text{mm}$ concrete cover are selected to evaluate the effect of concrete cover thickness and reinforcement ratio is slightly changed as $\rho_t=0.72\%$, $\rho_t=0.77\%$ and $\rho_t=0.83\%$ because only cover thickness changed for constant cross-section height. In the parametric study, cross-sectional dimensions of beams and constant moment span are selected similar with experiments. In all the cases 2D10-SD345 rebar has been arranged as compressive reinforcement while shear reinforcement is provided as per flexural strength requirement. Material properties in all the cases are similar as shown in Table 1.

3.3.1 Cracking pattern

Table 3 and Table 4 represents the analytical and design values of maximum crack space for the beams CN-SN, CN-SH and CH-SN, CH-SH respectively at yielding for all the cases of reinforcement ratio and concrete cover.

When normal strength concrete is used, the influence of high strength rebar is small. Almost in all the cases analytically observed crack space show safe values as compared to design value obtained from Eq. (1). Combination of high strength concrete with high strength rebar shows smaller crack space than other cases.

3.3.2 Comparison of analytically observed crack width with design values

Figs. 13 and 14 represents comparison of analytically observed crack width (W_a) with design values (W_d) obtained from Eq. (2) in case of various reinforcement ratios and concrete covers respectively.

Comparison between analytical and design values is provided at 0.9 times of yielding load.

Table 3. Crack space for beam CN-SN and CN-SH

Case	CN-SN		CN-SH	
	Ana.(mm)	L_{max} (mm)	Ana.(mm)	L_{max} (mm)
0.51% - C40	270	253	275	253
0.77% - C40	235	235	170	235
1.33% - C40	178	247	173	247
1.89% - C40	185	244	180	244
C20 - 0.72%	185	195	180	195
C60 - 0.83%	243	307	243	307

Table 4. Crack space for beam CH-SN and CH-SH

Case	CH-SN		CH-SH	
	Ana.(mm)	L_{max} (mm)	Ana.(mm)	L_{max} (mm)
0.51% - C40	313	221	265	221
0.77% - C40	180	209	178	209
1.33% - C40	180	216	143	216
1.89% - C40	198	213	168	213
C20 - 0.72%	198	170	168	170
C60 - 0.83%	313	268	238	268

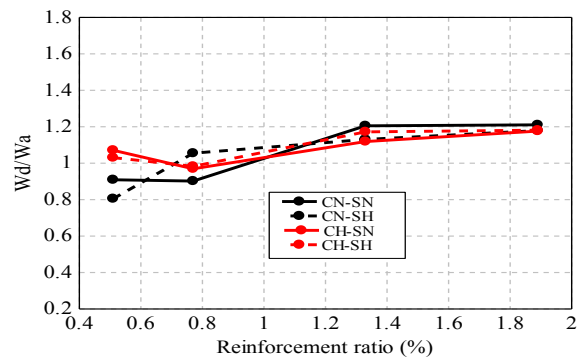


Fig.13 Comparison of crack width in case of reinforcement ratio

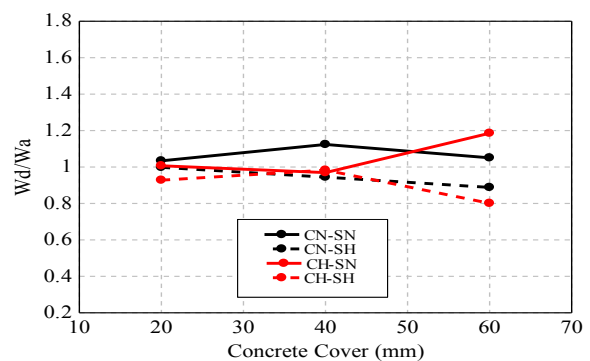


Fig. 14 Comparison of crack width in case of concrete cover

It is observed that the ratio of design values to analytical observed values progressively becomes slightly larger than unity with increase of reinforcement ratio.

In case of various concrete covers, the ratio of design values to analytical observed values is almost constant.

In all the cases of reinforcement ratio and concrete cover, for beams with high strength rebar along with either normal or high strength concrete, mostly analytically observed values for maximum crack width show reasonable values as compared to Eq. (2).

3.1.3 Comparison of analytically observed moment-curvature with design values

Figs. 15 and 16 represents comparison of analytically observed moment-curvature (MCa) with design values (MCd) obtained from Eq. (3) in case of various reinforcement ratios and concrete covers respectively. Comparison between analytical and design values is provided at 0.9 times of yielding load

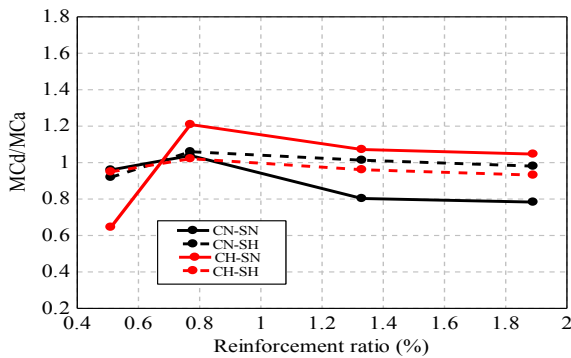


Fig.15 Comparison of moment-curvature in case of reinforcement ratio

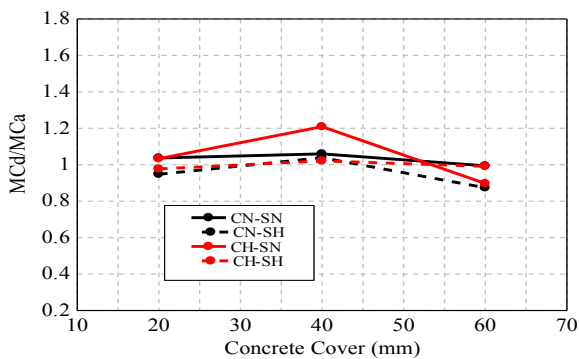


Fig. 16 Comparison of moment-curvature in case of concrete cover

In the case of various reinforcement ratios, for the beams with high strength rebar along with either normal or high strength concrete, the ratio of design values to analytically observed values remains almost unity. Similar trend has been observed for the cases of various concrete cover. For almost all the cases of beams with normal or high strength rebar along with either normal or high strength concrete, consistent analytical values has been observed as compared to design values obtained from Eq. (3).

4. SUMMARY AND CONCLUSION

An extensive experimental and analytical study was conducted to evaluate the effect of SD685 rebar on crack width, crack space and deformation behavior and following conclusions are drawn.

- (1) At higher stress levels of high strength rebar, experimentally as well as analytically observed maximum crack spaces and maximum crack widths are evaluated reasonably in comparison to JSCE's design equation for maximum crack space and maximum crack width.
- (2) At higher stress levels of high strength rebar, experimentally as well as analytically observed deformation behavior show consistent behavior with JSCE's design equation for moment-curvature.
- (3) RBSM can successfully evaluate the cracking and deformation behavior of RC beams comprising of high strength rebar.
- (4) JSCE's equation governing maximum crack width and deformation are applicable for rebar stress levels until SD685.

REFERENCES

- [1] Mast R.F.; Dawood, M.; Rizkalla, S.H.; and Zia, P., "Flexural Strength Design of Steel Beams with High Strength Steel Bars," *ACI Structural Journal*, V. 105, No. 5, Sept-Oct., pp. 570-577, 2008
- [2] Sumpter, M.S.; Rizkalla, S.H.; and Zia, P., "Behavior of High-Performance Steel as Shear Reinforcement for Concrete Beams," *ACI Structural Journal*, ASCE, V. 106, No. 2, Mar.-Apr., 171-177, 2009
- [3] Standard Specifications for Structures-2012, Design, JSCE, 2012
- [4] Marine et al. "High-Strength Flexural Reinforcement in Reinforced Concrete Flexural Members under Monotonic Loading" *ACI Structural Journal*, DOI: 10.14359/51688057, Nov.-2015
- [5] Shahrooz et al. "Flexural Members with High-Strength Reinforcement: Behavior and Code Implications" *American Society of Civil Engineers*, DOI: 10.1061/(ASCE)BE.1943-5592.0000571, 2011
- [6] Yamamoto, Y. et al., "Crack propagation analysis of reinforced concrete wall under cyclic loading using RBSM" *European Journal of Environmental and Civil Eng.*, 18(7), 2017, 780-792, 2014
- [7] Saito S., "Numerical analysis of reinforced concrete structures using spring network model" *Journal of Material, Concrete Structures and Pavements*, Japan Society of Civil Engineers, Np.627/V. 44, 289-303, 1999
- [8] Yamamoto. Y., Nakamura, H., Kuroda, I. and Furuya, N., "Analysis of compression failure of concrete by Three Dimensional Rigid Body Spring Model." *Journal of JSCE*, 64: 612-630, 2008 (in Japanese)
- [9] Suga, M., Nakamura, H., Higai, T. and Saito, S., "Effect of bond properties on the mechanical behavior of RC beam" *Proceedings of Japan Concrete Institute*, V. 23, No. 3, 295-300, 2001